Inorganic Ions Enhance the Number of Product Compounds through Heterogeneous Processing of Gaseous NO2 on an Aqueous Layer of Acetosyringone

Inorganic ions enhance the number of product compounds through heterogeneous processing of gaseous NO_2 on aqueous layer of acetosyringone

Pan Li[1,4], Hongwei Pang[1,2,3], Yiqun Wang[1,4], Huifan Deng[1,4], Jiangping Liu[1,4], Gwendal Loisel[1,2,3], Biao Jin[1,2,3], Xue Li[5], Davide Vione,[6] Sasho Gligorovski[1,2,3*]

[1]State Key Laboratory of Organic Geochemistry and Guangdong Provincial Key Laboratory of Environmental Protection and Resources Utilization, Guangzhou Institute of Geochemistry, Chinese Academy of Sciences, Guangzhou 510 640, China
[2]Guangdong-Hong Kong-Macao Joint Laboratory for Environmental Pollution and Control, Guangzhou Institute of Geochemistry, Chinese Academy of Science, Guangzhou 510640, China
[3]Chinese Academy of Science, Center for Excellence in Deep Earth Science, Guangzhou, 510640
[4]University of Chinese Academy of Sciences, Beijing, China
[5]Institute of Mass Spectrometry and Atmospheric Environment, Jinan University, Guangzhou 510632, China
[6]Dipartimento di Chimica, Università degli Studi di Torino, Via Pietro Giuria 5, 10125 Torino, Italy

* Correspondence to:

Sasho Gligorovski

gligorovski@gig.ac.cn

Abstract

Methoxyphenols represent important airborne pollutants which can participate in the generation of secondary organic aerosol (SOA) through chemical reactions with atmospheric oxidants. In this study, we assess the influence of ionic strength, pH, and temperature on the heterogeneous reaction of NO_2 with an aqueous film consisting of acetosyringone (ACS), as a model compound for methoxyphenols.

The uptake coefficient of NO_2 (50 ppb) on aqueous film of ACS (1×10^{-5} mol L^{-1}) measured by vertical wetted wall flow tube (VWWFT) reactor, is $\gamma = (9.3 \pm 0.09) \times 10^{-8}$ at pH 5, and increases by about one order of magnitude to $\gamma = (8.6 \pm 0.5) \times 10^{-7}$ at pH 11. The analysis performed by membrane inlet single photon ionization time of flight mass spectrometry (MI-SPI-TOFMS) reveals an increase in the number of product compounds and a change of their chemical composition upon addition of nitrate ions and sulfate ions to the aqueous layer consisting of ACS. A tentative mechanism is suggested for the formation of *m/z* 234 and 262 by addition of sulfate to a phenolic ring. These results suggest that inorganic ions may play an important role during the heterogeneous oxidation processes in the aqueous layer of the condensed aerosols.

Synopsis. Water-dissolved sulfate and nitrate affect the reaction between gas-phase NO_2 and an aqueous layer of acetosyringone, modifying both the reaction kinetics and the number and type of the reaction products.

1. Introduction

Biomass combustion including forest and grass fields as well as domestic burning for heating and cooking – represents a major source of lignin pyrolysis products. These include a variety of substituted methoxyphenols that may play a role in the formation of brown carbon in the atmosphere.[1-3] The important reactions of methoxyphenols include O_3, NO_3, Cl, and OH-initiated chemistry,[4-16] but the multiphase or heterogeneous chemistry of these compounds with NO_2[17, 18] is still unclear. We have chosen ACS as a proxy of methoxyphenols because field studies reported the emission rates of ACS as 28.1 and 55.3 mg kg^{-1} of burned oak and eucalyptus, respectively, which would give an important contribution to particle-phase emissions.[17] Evaluation of NO_2 heterogeneous and multiphase reactions and their effect on brown carbon and consequent haze formation processes should be paid more attention, especially in China where the NO_2 mixing ratios in the atmosphere are frequently high (40 to 50 ppb).[18, 19] For example, NO_2 can promote secondary organic aerosols (SOA) formation during oxidation of methoxyphenols by OH, resulting in the formation of organic nitrates.[20] Indeed, the oxidation processes of volatile organic compounds (VOCs) by hydroxyl radical (OH) and ozone (O_3) lead to the formation of SOA that is strongly dependent on nitrogen oxide concentration (NO_x).[21] Furthermore, the presence of NO_2 induces an increase in the mean diameter and number concentration of SOA particles,[20] and an increase in NO_2 levels from 40 to 109 ppbv was found to promote SOA formation.[20]

Ionic strength in liquid water of clouds differs substantially from that of aerosol particles.[21] The ionic strength in clouds ranges between 7.5×10^{-5} and 1×10^{-2} mol L^{-1},[22] while in urban aerosols it can easily reach values of up to 18.6 mol L^{-1}, and even 43 mol L^{-1} [22] during severe haze events. For this reason, the rates of heterogeneous reactions of atmospheric oxidants within the aqueous phase of aerosol particles will be affected by ionic strength and will differ

from that of cloud droplets.[15] For example, Kroll et al.[23] found that the enhanced uptake of glyoxal onto aqueous seed particles containing sulfate ions (SO_4^{2-}) and mixed SO_4^{2-}/H_2SO_4 was not a result of particle acidity but rather of ionic strength. Real-time measurements of aerosol particles indicated that most of them contain a mixture of organic compounds and SO_4^{2-}, with an organic to sulfate ratio of 1:1.[24] The average SO_4^{2-} concentration of clouds, fog and rainwater observed in southern California ranged between 9.4 and 475 mM.[25] Lately, the concentration of SO_4^{2-} has been found to decrease while the concentration of nitrate ions (NO_3^-) has been found to increase.[26, 27] The uptake coefficient of O_3 on ACS ([ACS] = 1×10^{-6} mol L^{-1}, pH 3) in aqueous solution increased by about one order of magnitude, from $\gamma = (1.39 \pm 0.38)\times10^{-7}$ in ultra-pure water to $\gamma = (1.17 \pm 0.01)\times10^{-6}$ in the presence of ionic strength adjusted with SO_4^{2-} (I = 0.9 mol L^{-1}).[15] On the other hand, the uptake coefficient of O_3 on aqueous ortho-vanillin at pH 5.6 increased from $\gamma = (1.9 \pm 0.1)\times10^{-7}$ in absence of added salts to $\gamma = (6.9 \pm 0.3)\times10^{-7}$ at I = 0.2 mol L^{-1} adjusted by SO_4^{2-}, and decreased again to $(2.0\pm0.1)\times10^{-7}$ at higher ionic strength values.[16]

Here, for the first time to our knowledge we assess the impact of sulfate and nitrate ions on the heterogeneous reactions of NO_2 with aqueous films consisting of ACS at pH 6, by use of a vertical wetted wall flow tube (VWWFT) reactor. The experimental pH 6 was chosen because of recent reports that typical pH values for cloud and fog droplets range between 2 and 7, while pH values for continental and marine aerosol particles exhibit a broader range, from 1 to 5 and from 0 to 8, respectively.[28] For example, in winter fog in Beijing pH ranges between 4.7 and 6.9.[29] Shi et al.[30] reported that nitrate and sulfate were the most prominent water soluble (WS) ions in the pH range 3-6. There is also evidence that the aqueous S(VI) concentrations increase by two orders of magnitude through S(IV)-NO_2 reaction for the pH range between 5.4 and 6.2.[31] In addition, the pH values of surface water (river, lake) usually range between 6 and 9.[32]

The formation of product compounds by the heterogeneous reactions of gaseous NO_2 with aqueous ACS, in absence and presence of NO_3^- and SO_4^{2-} was assessed by a membrane inlet single photon ionization time of flight mass spectrometer (MI-SPI-TOFMS). The presence of SO_4^{2-} had a tremendous impact on the number of products formed, the nature of which was altered upon addition of NO_3^- and SO_4^{2-} to the aqueous layer consisting of ACS.

2. Experimental

2.1 Experimental set-up

The heterogeneous reaction between gaseous NO_2 and an aqueous layer containing ACS, or a mixture of ACS with SO_4^{2-} or NO_3^- was assessed using a VWWFT (80 cm length and internal diameter (d) = 1.1 cm). The flow tube reactor was connected simultaneously to a NO_2 analyzer to follow the kinetics of NO_2 evolution, and to a MI-SPI-TOFMS to monitor the formation of the volatile organic compounds (VOCs). A pure NO_2 flow of 10 mL min^{-1} (0–10 mL min^{-1} mass flow controller, Seven Star, China) was mixed with 1000 mL min^{-1} air flow (0-500 mL min^{-1}, Seven Star, China) to obtain an atmospherically relevant NO_2 mixing ratio of 50 ppb. Gaseous NO_2 was introduced into the vertically aligned flow tube by a movable glass injector and the NO_2 concentrations were measured online at the exit of the flow tube by an NO_2 analyzer (Eco Physics, model CLD 88p) connected with a photolytic converter (Eco Physics, model PLC 860). The detection limit of the NO_x analyzer was 10 ppt with a time resolution of 1 s.[33-35]

The temperature in the flow tube reactor was held constant at 293 ± 0.02 K by temperature-controlled water circulating through its jacket, which was connected with a thermostated bath (Lauda, RC Germany). Aqueous solutions consisting of ACS ([ACS] = 1×10^{-5} mol L^{-1})

Commented [D1]: The range of the mass flow controller (0-500) does not match with the used flow (1000). Moreover, 10 mL to 1000 mL does not make 50 ppb (was pure NO2 really used, or was it already NO2 in air?).

(Sigma-Aldrich, 98.5%), or of ACS mixed with Na_2SO_4 (Sigma Aldrich, ≥ 99.0%) or $NaNO_3$ (Sigma Aldrich, ≥ 99.0%) were prepared with ultra-pure water (Sartorius 18 MΩ, H_2O-MM-UV-T, Germany). The pH values of these solutions were measured by a pH meter (Mettler Toledo). To simulate the pH of clouds, fog and moderately acidic particles, pH was adjusted to 6 by addition of HCl. Another reason for choosing pH 6 is that the measured uptake coefficients at pH values below 5 are extremely low, and thus not important in an atmospheric context (*vide infra*). The prepared aqueous solution containing either ACS, or a mixture of ACS with SO_4^{2-} or NO_3^- was continuously pumped into the reactor by a peristaltic pump (LabV1/MC4, SHENCHEN, China) with a flow of 5 mL min^{-1}. The Reynolds number was lower than 10 (Re = 0.2), indicating a laminar flow of the aqueous film in the reactor.[15]

2.2. Membrane inlet single photon ionization time of flight mass spectrometry (MI-SPI-TOFMS)

The membrane inlet single photon ionization time of flight mass spectrometer (MI-SPI-TOFMS) is a novel instrument aimed for continuous and online monitoring of VOCs. In this study, we used a commercial MI-SPI-TOF-MS instrument (SPIMS 3000, Guangzhou Hexin Instrument Co., Ltd., China) with mass resolution m/Δm 800-900, to observe the VOCs produced by the heterogeneous reaction of NO_2 with ACS, ACS/$NaNO_3$, and ACS/Na_2SO_4. The detailed explanation of MI-SPI-TOFMS is reported in previous papers,[36-39] thus description is kept short here. Briefly, SPIMS 3000 has 3 parts: (1) a membrane inlet system, with a 0.002-inch thick permeable membrane (dimethylsiloxane) (Technical Production, Inc., U.S.A.), the role of which is to accumulate VOCs; (2) a single photon ionization (SPI) source, equipped with a commercial deuterium lamp (Hamamatsu, Japan), and (3) a reflectron TOF-MS, containing a double-pulsed acceleration region, a field-free drift tube, a reflector and an

ion detector.[36] The raw data were processed by software (SPIMS 3000 V1.0.1.2.0, Guangzhou Hexin Instrument Co., Ltd., China).[36-39]

3. Results and Discussion

3.1. Estimation of NO_2 uptake coefficients

The uptake coefficient (γ) of NO_2 on aqueous solutions containing ACS, or a mixture of ACS with SO_4^{2-} or NO_3^- was calculated as follows:

$$\gamma = \frac{2r k_{1st} H_{NO_2} RT}{\bar{\nu}} \quad \text{(Eq-1)}$$

where $\bar{\nu}$ = 3.67×10^4 (cm s^{-1}) at the temperature T = 293 K is the average speed of NO_2, r = 0.55 cm is the internal radius of the flow tube, k_{1st} (s^{-1}) is the pseudo first-order rate constant for the reaction between NO_2 and ACS ($k_{1st} = k_{2nd}$ [ACS]), H_{NO2} is the Henry's law constant of NO_2 in a dilute aqueous solution (H_{NO2} = 1.4×10^{-2} M atm^{-1}),[40] and R = 8.314 J mol K^{-1}.

The k_{1st} value can be calculated by the pseudo-first order kinetic law as follows:

$$\ln\left(\frac{[NO_2]_t}{[NO_2]_0}\right) = -k_{1st} \cdot t \quad \text{(Eq-2)}$$

where ($[NO_2]_t/[NO_2]_0$) is the ratio between the NO_2 concentration at time t and the initial NO_2 concentration, and t is the residence time of gaseous NO_2 in the VWWFT reactor.

The heterogeneous reactivity will not occur across the entire liquid film but only at the surface, if the aqueous-phase reaction is fast enough compared to the diffusion of gaseous NO_2 into the liquid phase.[41] When the kinetics is controlled by aqueous-phase diffusion,[15, 42-45] the uptake coefficient of NO_2 can be estimated as follows:

$$\gamma = \frac{4H_{NO_2}RT\sqrt{k_{1st}D_{aq}}}{\bar{v}} \quad \text{(Eq-3)}$$

Considering that $k_{1st} = k_{2nd}[ACS]$, Eq-3 becomes:

$$\gamma = \frac{4H_{NO_2}RT\sqrt{k_{2nd}[ACS]D_{aq}}}{\bar{v}} \quad \text{(Eq-4)}$$

where D_{aq} is the diffusion coefficient of NO_2 in dilute aqueous solutions ($D_{aq} = 1.23\times10^{-5}$ cm^2 s^{-1}).[40] The aqueous film was uniform without ripples and was flowing under laminar conditions, according to the estimated Reynolds number (Re) = 0.25.[42]

Figure 1 shows the dependence of the NO_2 uptake coefficients on the square root of the concentration of ACS, according to Eq-4.

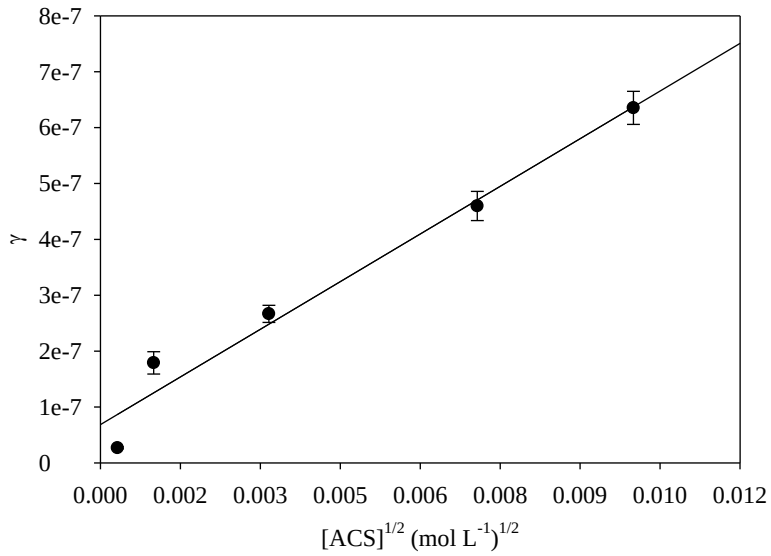

Figure 1: The uptake coefficients of NO_2 (50 ppb) as a function of the square root of ACS concentration in the aqueous phase. The solid line shows the fit according to Eq-4

The linear dependence between γ and $\sqrt{[ACS]}$ indicates that the uptakes are effectively and exclusively driven by the chemical reaction of NO_2 with ACS in the aqueous phase at pH 6.[46]

The combination of the slope depicted in Figure 1 and Eq-4, gives the second-order rate constant (k_{2nd}) = 2.6 × 10^5 M^{-1} s^{-1} for the reaction between NO_2 and ACS in the aqueous phase at pH 6. The obtained k_{2nd} is of the same order of magnitude as the second-order rate constants for the reactions of NO_2 with syringol, catechol and guaiacol in the aqueous phase at pH 6.[46] The estimated k_{2nd} is also similar to the second-order rate constant of O_3 with lignin-derived compounds in the bulk aqueous phase (k_{2nd} = 2.7 × 10^5 M^{-1} s^{-1}),[47] and it is about two times slower than the rate constant (k_{2nd} = 5.4 × 10^5 M^{-1} s^{-1}) for the reaction of O_3 (100 ppb) with ortho-vanillin ([o-VL] = 1×10^{-5} mol L^{-1} at pH 5.6.[16]

However, it has to be considered that the uptake coefficients are measured on relatively thick liquid films compared to the liquid film occurring on aerosol particles. The diffuso-reactive length (l) expressed in meters (m) is a measure of the distance from the interface in which the reaction occurs [42]:

$$l = \sqrt{\frac{D_{aq}}{k_{1st}}} \qquad \text{(Eq-5)}$$

Under the experimental conditions applied in this study, l varies between 1.3 × 10^{-4} m and 2.2 × 10^{-4} m. The diffuso-reactive parameter, q, is a dimensionless parameter that can be estimated as follows:[41]

$$q = a\sqrt{\frac{k_{1st}}{D_{aq}}} = \frac{a}{l} \qquad \text{(Eq-6)}$$

where a is the radius of the aerosol particle.

Hanson et al. (1994) have shown that the effective uptake coefficients occurring on small particles are related to the measured uptakes on thick liquid films under laboratory conditions, as follows:

$$\gamma_e \cong \left(\coth q - \frac{1}{q}\right)\gamma \qquad \text{(Eq-7)}$$

where $\left(\coth q - \frac{1}{q}\right)$ is the correction factor that must be applied to extrapolate the measured uptake coefficients to small atmospheric particles.

When *l* is small compared to *a*, the correction factor is ~ 1 implying that the measured uptake coefficients in the laboratory can be applied to small particles.[41, 48] The atmospheric implications are discussed in section 3.6.

When adding Na_2SO_4 or $NaNO_3$ to an aqueous solution containing ACS, the Henry's law coefficient of NO_2 needs to be corrected by the Setchenow equation that considers the ionic strength effect.[24,28,49] The procedure for the calculation of the Henry's law coefficients of NO_2 (H_{NO2}) at different ionic strengths is similar to that for H_{O3} that was previously reported.[15, 16] Briefly, the estimation of the Henry's law constants of gases in aqueous salt solutions as a function of temperature can be calculated as follows:[15, 16]

$$\log\left(\frac{H}{H_0}\right) = \sum_i (h_i + h_{G,0} + h_T(T - 298.15K))c_s \qquad \text{(Eq-8)}$$

The calculated values of H_{NO2} at different ionic strengths adjusted by Na_2SO_4 and $NaNO_3$ are shown in Table S1.

3.2. Ionic strength effect on the NO_2 uptakes

The presence of inorganic ions in the aerosol particles can influence the uptake coefficients of atmospheric oxidants (e.g. O_3, NO_2) with organic compounds. The product compounds that are formed upon these heterogeneous reactions can be also affected by ionic strength.[15, 42, 49-53] Therefore, the uptake coefficients of NO_2 on aqueous films containing ACS were measured in the absence of inorganic ions and in the presence of different ionic strengths adjusted by Na_2SO_4 or $NaNO_3$. Adding Na_2SO_4 to an aqueous solution of ACS influences pH due to deprotonation[15] (Table S2). The pH of the aqueous solution containing either ACS, a mixture of ACS/$NaNO_3$ or of ACS/Na_2SO_4 was fixed at 6, to enable the comparison of the uptake

coefficients in the same pH conditions corresponding to cloud droplets (absence of inorganic ions) and aerosol particles (presence of SO_4^{2-} or NO_3^-).

The uptake coefficient of NO_2 on aqueous ACS in the absence of inorganic ions is $\gamma = (2.6 \pm 0.2)\times10^{-7}$. This value is of the same order of magnitude as the uptake coefficients of NO_2 (80-100 ppb) on resorcinol (10^{-4} mol L^{-1}) and guaiacol (10^{-4} mol L^{-1}) at pH 6.[44,46] One then observes an increase by ca. 2 times to $\gamma = (4.7 \pm 0.2)\times10^{-7}$ at ionic strength I = 0.09 mol L^{-1}, adjusted by SO_4^{2-} ions (Figure 2). The further increase of ionic strength up to 4.5 mol L^{-1} leads to a decrease of the uptake coefficient to $\gamma = (3.7 \pm 0.3)\times10^{-7}$. Similar behavior of the uptake coefficients with ionic strength has been previously observed for the heterogeneous reaction of O_3 with ortho-vanillin.[16]

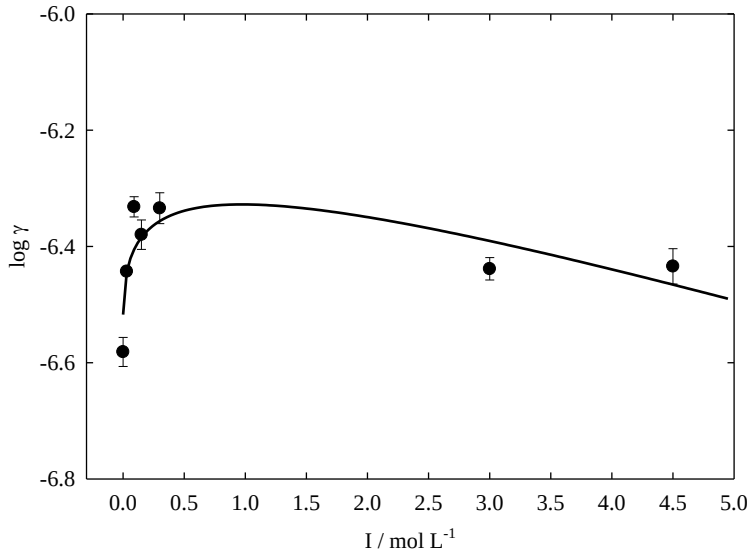

Figure 2: Uptake coefficients of NO_2 (50 ppb) on aqueous ACS ([ACS] = 1×10^{-5} mol L^{-1}), plotted as a function of ionic strength adjusted by SO_4^{2-} ions. The error bars of the uptake coefficients represent ± 2σ. The solid curve represents data fit with Eq-10.

A Debye-Huckel-Brønsted-Davies equation including the hypothesis of Guggenheim can properly describe the rise of the rate coefficients with increasing ionic strength, up to I ≈ 0.5 M, as follows:[54-56]

$$\log k_{1st} = \log k_{1st}(I \to 0) + A\frac{\sqrt{I}}{1+\sqrt{I}} + F_{ij}c_{ij} \quad \text{(Eq-9)}$$

where I is the ionic strength of the solution adjusted by SO_4^{2-} ions, A is a given experimental parameter (A = 0.51 for water at T = 293 K), F_{ij} is a variable kinetic parameter, and c_{ij} is the concentration of SO_4^{2-} ions.

The uptake coefficient of NO_2 defined by Eq-1 can be expressed by the Debye-Huckel-Brønsted-Davies-Guggenheim equation by replacing k_{1st} from Eq-9 into Eq-1, and by taking logarithm of both sides of the equation. In this way, Eq-10 is obtained which predicts the behavior of the uptake coefficients of NO_2 at ionic strengths values higher than 0.5 M. [16]

$$\log\gamma = \log(2rH) + \log\left(\frac{k_{1st}(I\to 0)}{\bar{v}}\right) + A\frac{\sqrt{I}}{1+\sqrt{I}} + F_{ij}c_{ij} \quad \text{(Eq-10)}$$

where H is the dimensionless Henry constant of NO_2 at different ionic strength values adjusted by Na_2SO_4 (Table S1). The sharp increase of the uptake coefficients of NO_2 at lower ionic strength values up to 0.5 M (Figure 2) can be ascribed to the catalytic effect caused by SO_4^{2-}, which has been highlighted in previous studies.[16, 57, 58] The further increase of the ionic strength adjusted by SO_4^{2-} leads to decreasing NO_2 uptake coefficients, which is described by the higher-order empirical term $F_{ij}c_{ij}$ that can be obtained numerically from the fit of log γ vs. I by Eq-10. The modeled F_{ij} = 0.042±0.007 describes the dependence on the ionic strength (adjusted by SO_4^{2-}) of the uptake coefficient of NO_2 on an aqueous film consisting of ACS. Figure 3 shows the effect of NO_3^- on the uptake coefficients of NO_2 on aqueous ACS. Because $NaNO_3$ is not completely dissociated in aqueous solution, the effective ionic strength (I_{eff}) was estimated (Eq-11) by using the association equilibrium constant of $NaNO_3$: K ($NaNO_3/Na^+$, NO_3^-) = 1.73 M^{-1} at T = 293 K.[59, 60]

$$I_{eff} = \sqrt{\frac{[NaNO_3]}{K} + \frac{0.25}{K^2}} - \frac{1}{2K} \quad \text{(Eq-11)}$$

Figure 3 shows that the uptake coefficients of NO_2 decrease with increasing ionic strength adjusted with NO_3^-, from $\gamma = (2.6 \pm 0.8)\times10^{-7}$ in the absence of $NaNO_3$ to $\gamma = (1.7 \pm 0.1)\times10^{-7}$ at I_{eff} = 0.03 mol L^{-1}.

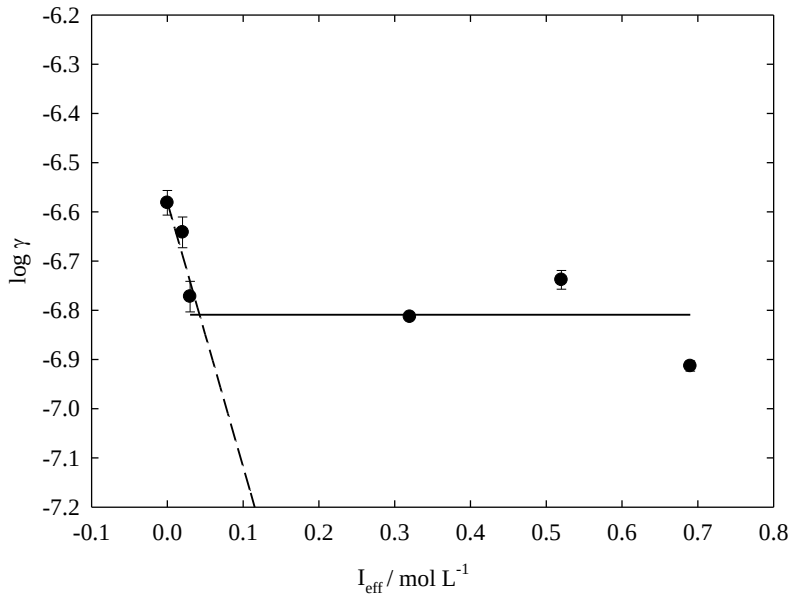

Figure 3: The dependence of the uptake coefficients of NO_2 (50 ppb) on aqueous ACS ([ACS] = 1×10^{-5} mol L^{-1}), with ionic strength adjusted by NO_3^-. The error bars of the uptake coefficients are 2σ. The dashed line is the fit of the experimental data with Eq-13.

A further increase of the ionic strength up to I_{eff} = 0.7 mol L^{-1} leads to a saturation effect of the uptake coefficients (Figure 3). The linear dependence of the rate constants k_{1st} with I_{eff} can be defined by Eq-12.[59]

$$\log K_{1st} = \log[K_{1st}(I_{eff} \to 0)] + bI_{eff} \quad \text{(Eq-12)}$$

where b is the kinetic salting coefficient that governs the acceleration or the deceleration of the reaction rate.[22, 59] Considering the link between k_{1st} and γ, the combination of Eq-3 and Eq-12 yields Eq-13 that describes the dependence of the uptake coefficients on the ionic strength in the case of $NaNO_3$: [16]

$$\log\gamma = \log(2rH) + \log\left(\frac{k_{1st}(I\to 0)}{\bar{v}}\right) + bI \qquad \text{(Eq-13)}$$

where H is the dimensionless Henry constant of NO_2 at different ionic strength values adjusted by NO_3^- (Table S1). The fit of log γ with the ionic strength, shown in Figure 3, yields b = -5.4 L mol^{-1} that is similar to b = -1.7 L mol^{-1} from a previous study focused on the effect of ionic strength on the uptake coefficients of ozone on o-VL.[16] However, the slope depicted in Figure 3 is steeper compared to that by Wang et al.,[16] implying that in the oxidation of ACS by NO_2 the deceleration of the reaction with increasing ionic strength (NO_3^-) is faster than in the case of O_3 + o-VL. Interestingly, the photochemical degradation of vanillin was also decelerated (b = -0.4 L mol^{-1}) by increasing ionic strength adjusted by NO_3^-.[61] These results suggest that heterogeneous oxidation and photochemical degradation of methoxyphenols would be slowed down in the presence of nitrate ions in aerosol deliquescent particles, compared to the corresponding degradation in cloud water.

3.3. Effect of pH

The uptake coefficients of NO_2 were assessed as a function of pH in the absence of added salts. The pH dependence of the uptakes of NO_2 shown in Figure 4 is associated with the protonation/deprotonation equilibrium of ACS.[15] Ammann et al.[46] reported similar behavior of the uptake coefficients of NO_2 on aqueous layers consisting of guaiacol, syringol and catechol at different pH values ranging from 1 to 13, which was ascribed to the increasing fraction of the deprotonated species at higher pH.

Figure 4 shows that, at pH values below the pKa of ACS (7.8 ± 0.2),[62] the heterogeneous reactivity of NO_2 on ACS is slowed down. The lowest measured uptake coefficient of NO_2 on aqueous ACS was observed at pH 5 ($\gamma = (9.3 \pm 0.09) \times 10^{-8}$).

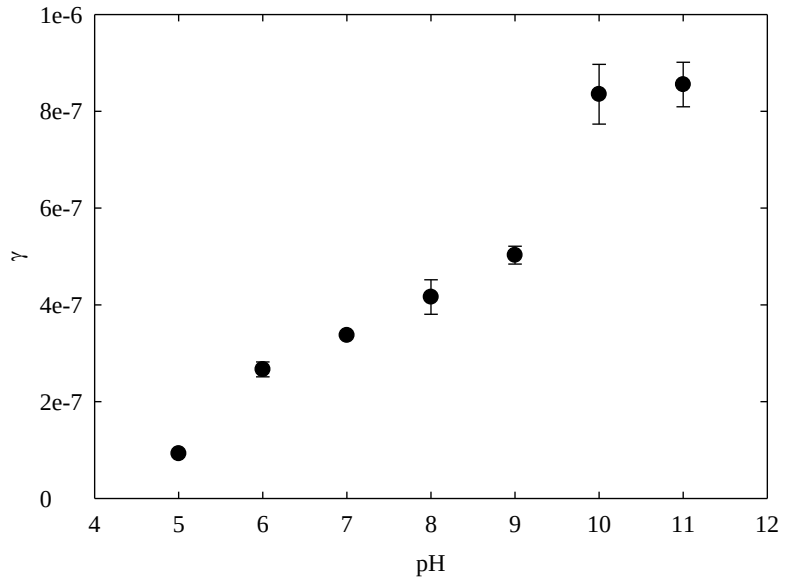

Figure 4: Uptake coefficients of NO_2 (50 ppb) as a function of pH in the absence of added salts. The error bars represent 2σ, resulting from the statistical error on the slope of the regression line obtained by Eq-2 that represents the first-order rate constant, k_{1st}.

At pH < 5 the uptake coefficients of NO_2 were not measurable, indicating that the reaction of gas-phase NO_2 with ACS within highly acidic particles would be extremely slow and would not be important from an atmospheric point of view.

At pH values lower than the pKa, the reaction of ACS with NO_2 proceeds by electron transfer (R-1) producing nitrite ion (NO_2^-), followed by deprotonation of the aromatic radical cation (proton-coupled electron transfer).[63, 64]

$C_{10}H_{11}O_3\text{-}OH + NO_2 \rightarrow C_{10}H_{11}O_3\text{-}OH^+ + NO_2^-$ (R-1)

The rate of reaction R-1 depends on the charge density in the aromatic ring and, therefore, on the electron donor capacity of the substituent.[64]

At pH values higher than the pKa, the phenolic group of ACS is ionized and its reaction with NO_2 is much faster because it occurs most likely through a pure electron transfer mechanism:

$C_{10}H_{11}O_3\text{-}O^- + NO_2 \rightarrow C_{10}H_{11}O_3\text{-}O^\bullet + NO_2^-$ (R-2)

Under alkaline conditions (pH 8) that are typical of surface waters (river, lake)[32] and marine aerosol particles,[28] the uptake coefficient of NO_2 increased by 6 times up to $\gamma = (5.4 \pm 0.3)\times10^{-7}$ compared to the uptake coefficient at pH 5. In addition, it has to be noted that the pH values of marine aerosols can be highly variable (pH 0-8) depending on their size, but the pH value of nascent submicron sea-spray aerosols can be significantly lower (pH 4) than that of sea water (pH 8).[65] A further increase of pH caused an increase of γ by about one order of magnitude: it was $\gamma = (1.0 \pm 0.1)\times10^{-6}$ at pH 10, compared to $\gamma = (9.3 \pm 0.09)\times10^{-8}$ measured at pH 5.

The behavior and the values of the uptake coefficients of NO_2 shown in Figure 4 are in good agreement with the uptake coefficients of O_3 on ACS at different pH values, indicating similar reactivity independently of the oxidant.[15]

3.4. Effect of temperature

The reaction of NO_2 on aqueous ACS at pH 6 was studied at four different temperatures, ranging from 288.15 K to 318.15 K, in the absence of inorganic ions as well as at I = 3 mol L^{-1} adjusted by SO_4^{2-}, and at I_{eff} = 0.5 mol L^{-1} (NO_3^-) (Figure 5). The reaction rate of NO_2 in a dilute aqueous-phase containing ACS increased by three times when temperature changed from 288.15 K to 318.15 K, while in the presence of inorganic ions the rate only slightly decreased (note that, in Figure 5, k_{1st} is plotted versus T^{-1}).

The activation energy E_A of the reaction between NO_2 and ACS was estimated by Arrhenius law, as follows:

$$k_{1st} = A\exp\left(\frac{-E_A}{RT}\right) \quad \text{(Eq-14)}$$

where A is the pre-exponential factor, and $-E_A/R$ is the slope of the regression lines depicted in Figure 5. Considering the value of the gas constant R (8.314 J mol^{-1} K^{-1}), from the slope one obtains E_A that is the activation energy of the reaction.

The linear fit (solid regression line) depicted in Figure 5 allows to estimate the activation energy E_A= 29 kJ mol^{-1} for the reaction of NO_2 with ACS in the absence of inorganic ions. This result indicates that a high activation energy is needed for R-1 (pH 6) to proceed.

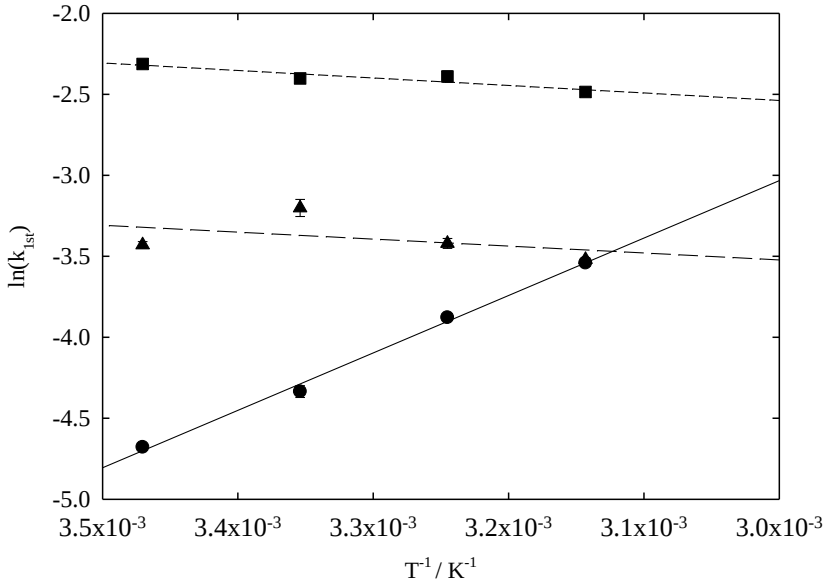

Figure 5: First-order rate constant (k_{1st}) of NO_2 (50 ppb) on aqueous ACS, as a function of temperature, at pH 6: ●) in the absence of inorganic ions; ■) at I = 3 mol L^{-1} (SO_4^{2-}), and ▲) at I_{eff} = 0.5 mol L^{-1} (NO_3^-). The errors bars represent ± 2σ, resulting from the statistical error on the slope of the regression line obtained by Eq-2, which represents the first-order rate constant, k_{1st}.

The obtained value of E_A in this study is similar to E_A = 39 kJ mol^{-1} for the reaction of NO_2 with aromatic compounds (anthrarobin).[66] A slightly negative temperature dependence was observed for the reaction of NO_2 with ACS in the presence of SO_4^{2-} and NO_3^-, which suggests that an increase in temperature slightly decreases the reactivity of NO_2 with the liquid film of ACS in presence of sulfate and nitrate ions.

3.5. Volatile Product Compounds Detected by MI-SPI-TOFMS Analysis

The formation of the compounds produced by heterogeneous reactions of NO_2 with ACS, ACS/NO_3^-, and ACS/SO_4^{2-} was observed on-line and continuously by MI-SPI-TOF-MS coupled to the VWWFT reactor. In the presence of nitrate ions it was I_{eff} = 0.09 M and, in the presence of sulfate ions, I = 0.3 M. These ionic strength values were chosen because they correspond to the maximum effects on the uptake coefficients of NO_2 caused by the presence of sulfate and nitrate as shown in Figure 2 and Figure 3, respectively. Figures S1-S3 display the signal intensities obtained from scans of mass to charge ratios (*m/z*) ranging between 50 and 250 amu, which correspond to the monitored products formed upon reaction of NO_2 with ACS, ACS/NO_3^-, and ACS/SO_4^{2-}, respectively. Figures S2 and S3 show clusters of peaks separated by regular mass units of Δ *m/z* 14 and 16 Da that correspond to CH_2 and O, respectively, and suggest a grouping of monomer units.[39, 67-69]

To statistically determine the significance of the observed product compounds compared to a blank experiment, data were examined by the Student t test with significance threshold $p < 0.05$ [70, 71]. The compounds with $p < 0.05$ were thus considered as potential products generated during the heterogeneous reactions of NO_2 with ACS, in the absence and in the presence of nitrate and sulfate ions.

Tentatively, three products were identified during the heterogeneous reaction of NO_2 with ACS. The formation profiles of *m/z* 78, *m/z* 135, and *m/z* 260 are shown in Figure S4. Typical profiles of compounds having *m/z* 234, 246, and 262, generated through heterogeneous reaction of NO_2 with ACS/SO_4^{2-} are shown in Figure 6.

The presence of inorganic ions in the aqueous solution led to a higher number of detected organic compounds upon reaction of gaseous NO_2 with aqueous films of ACS. The number of detected products rose up to ten in the presence of NO_3^-, while fifteen products were detected in the presence of SO_4^{2-}.

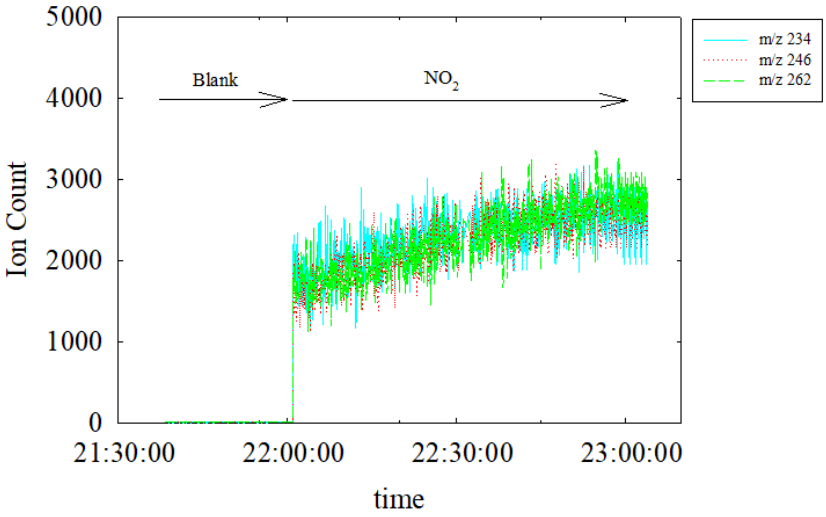

Figure 6: Typical profiles of compounds formed upon heterogeneous reactions of NO_2 with ACS in the presence of SO_4^{2-}.

The reaction product with *m/z* 260 was detected all three reaction systems, i.e., in absence of salt and in the presence of both sulfate and nitrate ions. However, the intensity of the signal decreased substantially in the presence of inorganic ions. The tentative reaction mechanism

for the formation of *m/z* 260 in absence of sulfate and nitrate ions is depicted in Scheme S1. The reaction product with *m/z* 246 was detected only in presence of nitrate and sulfate ions (Scheme S2). Finally, two reaction products with *m/z* 234 and 262 were formed only in presence of sulfate ions. Their tentative formation pathways are suggested in Scheme 1 and Scheme S3, respectively. The presence of nitrate anions in the aqueous ACS film induced the formation of several new compounds (*m/z* 118, 204, 206, 222, and 246) (Figure S2), including some molecules bearing a nitro group.

The number of detected product compounds increased even more when sulfate ions were present in the aqueous film of ACS. Compared to the compounds formed by reaction of NO_2 with ACS and ACS/NO_3^-, several new peaks appeared upon reaction of NO_2 with ACS/SO_4^{2-} (*m/z* 48, 62, 70, 156,220, 234, 248, 262 and 276) (Figure S3).

Tentative structures and aqueous-solution formation schemes could be hypothesized for the detected intermediates having *m/z* 234, 246, 260 and 262 (see Schemes 1 and S1-S3). The nitration reaction involving ACS + NO_2 is expected to follow the typical nitration pathway of phenols in water, where NO_2 first oxidizes the substrate to the corresponding phenoxy radical (reaction R-1 followed by deprotonation of the radical cation, or reaction R-2), and the nitroderivative is then produced by reaction between the phenoxy radical and another NO_2 molecule.[72] Note that NO_2 would sometimes react as a nitrating agent as described, and sometimes as an oxidant that is involved in demethylation and/or deacetylation processes.

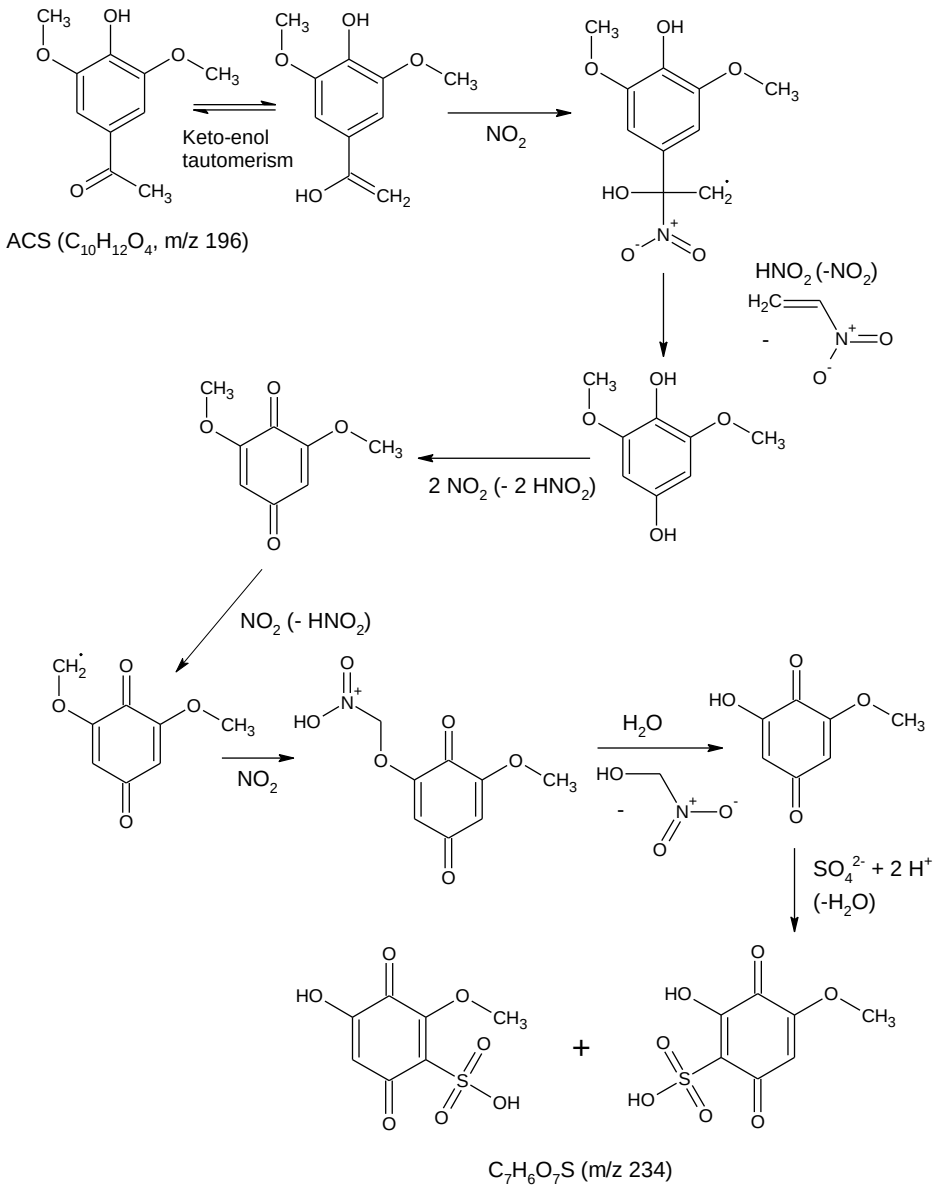

Scheme 1. Tentative proposed reaction pathways to account for the formation of the intermediate with *m/z* 234 during the heterogeneous reaction of NO_2 with ACS in presence of sulfate ions.

The loss of the acetyl group of ACS (H_3C-CO-, hypothesized to occur for *m/z* 234, 246 and 260) could be a consequence of the keto-enol tautomerism, which increases the reactivity of acetylic α-methyl towards oxidation reactions. Finally, we also suggest that the formation of *m/z* 234 and 262 may involve addition of sulfate to the aromatic ring of phenolic compounds. This kind of process might partially explain why the system ACS/NO_2/SO_4^{2-} produced more intermediates compared to ACS/NO_2, and it could also explain why addition of SO_4^{2-} accelerated the uptake of NO_2, at least until I = 0.09 mol L^{-1}. Direct involvement of NO_3^- in the formation of the relevant intermediates (e.g., *m/z* 246) seems unlikely from a mechanistic point of view, which could be supported by the lack of NO_2 uptake acceleration in the presence of NO_3^-. However, the ionic strength increase upon addition of NO_3^- might produce a salting-out effect that favors the transfer of aqueous-phase products to the gas phase, thereby facilitating their detection by MI-SPI-TOF-MS.

3.6. Atmospheric implications

The atmospheric lifetimes of ACS based on its reaction with gaseous NO_2, in absence and in presence of NO_3^- and SO_4^{2-} were calculated as follows:[15,16,43,44]

$$\tau = \frac{4N_{tot}}{\gamma \bar{v}[NO_2]_g} \qquad \text{(Eq-15)}$$

Where N_{tot} is the surface concentration of ACS expressed in molecules cm^{-2}, $\bar{v}$ is the mean velocity of NO_2 (cm s^{-1}), and $[NO_2]_g$ is the gas-phase concentration of NO_2 (molecules cm^{-3}). Based on previous studies the assumption is that N_{tot} = 10^{14} cm^{-2}.[43,44] We considered an average NO_2 concentration $[NO_2]_g$ = 4.9×10^{11} molecules cm^{-3} which corresponds to 20 ppb. The atmospheric lifetimes of ACS due to the night-time reactions with NO_2 in presence and absence of NO_3^- and SO_4^{2-} at pH 6 are summarized in Table 1.

Table 1: Lifetimes of ACS due to its reaction with gaseous NO_2 in absence and in presence of inorganic ions (typical values for NO_3^- and SO_4^{2-} in aerosols are here considered[22].

ACS	NO_3^-	SO_4^-	γ	γ_e	τ
mol L^{-1}	mol L^{-1}	mol L^{-1}	unitless	unitless	h
1×10^{-5}			2.67×10^{-7}	1.60×10^{-7}	38
1×10^{-5}	0.1		2.56×10^{-7}	6.90×10^{-8}	90
1×10^{-5}		0.02	6.14×10^{-7}	3.20×10^{-7}	19

For these calculations we used Eqs-6,7 to correct the measured uptake coefficients by assuming an aerosol particle with diameter of 1 μm. The corrected uptakes are summarized in Table 1.

It has to be noted that for particles with diameter larger than 1 μm the correction factor is ~ 1 and the measured uptake coefficients can be considered for estimation of the lifetimes without correction. In this case the lifetime of ACS would be 23 h in absence of inorganic ions, while in presence of nitrate and sulfate ions it would be 24h and 10h, respectively. These results suggest that inorganic anions such as NO_3^- and SO_4^{2-} can substantially affect the heterogeneous reaction of NO_2 with methoxyphenols in the condensed aerosol particles. The number of products that are formed upon reaction of ACS with NO_2 increase depending on the added inorganic anions. The chemical composition of the formed product compounds is also altered as a function of the amount and type of ionic strength: for example, organosulfate compounds are likely intermediates in the presence of SO_4^{2-} during the reaction of NO_2 with ACS and, potentially, with other methoxyphenols. The detected products are all highly oxygenated compounds with molecular mass that is often higher than that of ACS, which can have implications for SOA formation processes. Indeed, it has been shown that highly

oxygenated compounds in the gas-phase contribute to the formation of SOA, in particular by participating to the growth of new particles.

Associated content

Acknowledgment

This study was financially supported by the Chinese Academy of Science, International Cooperation Grant (N°: 132744KYSB20190007), National Natural Science Foundation of China (N°: 41773131, and N°: 41977187), State Key Laboratory of Organic Geochemistry, Guangzhou Institute of Geochemistry (SKLOG2020-5, and KTZ_17101) and National Key Research and Development Program (2017YFC0210103).

Supporting Information

Additional 2 tables, 6 figures, and 3 reaction schemes. The supporting information is available free of charge via the Internet on the ACS Publications website at http://pubs.acs.org.

Author information

Corresponding Author

* Phone: +86 2085291497; Email: gligorovski@gig.ac.cn

Notes

The authors declare no competing financial interest.

References

(1) Schauer, J. J.; Cass, G. R., Source Apportionment of Wintertime Gas-Phase and Particle-Phase Air Pollutants Using Organic Compounds as Tracers. *Environ. Sci. Technol.* **2000,** *34*, (9), 1821-1832.

(2) Bruns, E. A.; El Haddad, I.; Slowik, J. G.; Kilic, D.; Klein, F.; Baltensperger, U.; Prévôt, A. S. H., Identification of significant precursor gases of secondary organic aerosols from residential wood combustion. *Sci. Rep.* **2016,** *6*, (1), 27881.

(3) O'Neill, E. M.; Kawam, A. Z.; Van Ry, D. A.; Hinrichs, R. Z., Ozonolysis of surface-adsorbed methoxyphenols: kinetics of aromatic ring cleavage vs. alkene side-chain oxidation. *Atmos. Chem. Phys.* **2014,** *14*, (1), 47-60.

(4) Jammoul, A.; Gligorovski, S.; George, C.; D'Anna, B., Photosensitized Heterogeneous Chemistry of Ozone on Organic Films. *J. Phys. Chem. A* **2008,** *112*, (6), 1268-1276.

(5) Coeur-Tourneur, C.; Cassez, A.; Wenger, J. C., Rate Coefficients for the Gas-Phase Reaction of Hydroxyl Radicals with 2-Methoxyphenol (Guaiacol) and Related Compounds. *J. Phys. Chem. A* **2010,** *114*, (43), 11645-11650.

(6) Liu, C.; Zhang, P.; Wang, Y.; Yang, B.; Shu, J., Heterogeneous reactions of particulate methoxyphenols with NO3 radicals: Kinetics, products, and mechanisms. *Environ. Sci. Technol.* **2012,** *46*, (24), 13262.

(7) Lauraguais, A.; Bejan, I.; Barnes, I.; Wiesen, P.; Coeur-Tourneur, C.; Cassez, A., Rate Coefficients for the Gas-Phase Reaction of Chlorine Atoms with a Series of Methoxylated Aromatic Compounds. *J. Phys. Chem. A* **2014,** *118*, (10), 1777-1784.

(8) Zein, A. E.; Coeur, C.; Obeid, E.; Lauraguais, A.; Fagniez, T., Reaction Kinetics of Catechol (1,2-Benzenediol) and Guaiacol (2-Methoxyphenol) with Ozone. *J. Phys. Chem. A* **2015,** *119*, (26), 6759-6765.

(9) Sun, Y.; Xu, F.; Li, X.; Zhang, Q.; Gu, Y., Mechanisms and kinetic studies of OH-initiated atmospheric oxidation of methoxyphenols in the presence of O2 and NOx. *Phys. Chem. Chem. Phys.* **2019,** *21*, (39), 21856-21866.

(10) He, L.; Schaefer, T.; Otto, T.; Kroflič, A.; Herrmann, H., Kinetic and Theoretical Study of the Atmospheric Aqueous-Phase Reactions of OH Radicals with Methoxyphenolic Compounds. *J. Phys. Chem. A* **2019,** *123*, (36), 7828-7838.

(11) Zhang, T.; Yang, W.; Han, C.; Yang, H.; Xue, X., Heterogeneous reaction of ozone with syringic acid: Uptake of O3 and changes in the composition and optical property of syringic acid. *Environ. Pollut.* **2020,** *257*, 113632.

(12) Mekic, M.; Wang, Y.; Loisel, G.; Vione, D.; Gligorovski, S., Ionic Strength Effect Alters the Heterogeneous Ozone Oxidation of Methoxyphenols in Going from Cloud Droplets to Aerosol Deliquescent Particles. *Environ. Sci. Technol.* **2020,** *54*, (20), 12898-12907.

(13) Wang, Y.; Mekic, M.; Li, P.; Deng, H.; Liu, S.; Jiang, B.; Jin, B.; Vione, D.; Gligorovski, S., Ionic Strength Effect Triggers Brown Carbon Formation through Heterogeneous Ozone Processing of Ortho-Vanillin. *Environ. Sci. Technol.* **2021,** *55*, (8), 4553-4564.

(14) Net, S.; Gligorovski, S.; Pietri, S.; Wortham, H., Photoenhanced degradation of veratraldehyde upon the heterogeneous ozone reactions. *Phy. Chem. Chem. Phy.* **2010,** *12*, (27), 7603-7611.

(15) Net, S.; Nieto-Gligorovski, L.; Gligorovski, S.; Wortham, H., Heterogeneous ozonation kinetics of 4-phenoxyphenol in the presence of photosensitizer. *Atmos. Chem. Phys.* **2010,** *10*, (4), 1545-1554.

(16) Net, S.; Alvarez, E. G.; Gligorovski, S.; Wortham, H., Heterogeneous reactions of ozone with methoxyphenols, in presence and absence of light. *Atmos. Environ.* **2011,** *45*, (18), 3007-3014.

(17) Gutzwiller, L.; George, C.; Rössler, E.; Ammann, M., Reaction Kinetics of NO_2 with Resorcinol and 2,7-Naphthalenediol in the Aqueous Phase at Different pH. *J. Phys. Chem. A* **2002,** *106*, (50), 12045-12050.
(18) Ammann, M.; Rossler, E.; Strekowski, R.; George, C., Nitrogen dioxide multiphase chemistry: uptake kinetics on aqueous solutions containing phenolic compounds. *Phys. Chem. Chem. Phys.* **2005,** *7*, (12), 2513-8.
(19) Schauer, J. J.; Kleeman, M. J.; Cass, G. R.; Simoneit, B. R. T., Measurement of Emissions from Air Pollution Sources. 3. C1−C29 Organic Compounds from Fireplace Combustion of Wood. *Environ. Sci. Technol.* **2001,** *35*, (9), 1716-1728.
(20) Nie, W.; Ding, A. J.; Xie, Y. N.; Xu, Z.; Mao, H.; Kerminen, V. M.; Zheng, L. F.; Qi, X. M.; Huang, X.; Yang, X. Q.; Sun, J. N.; Herrmann, E.; Petäjä, T.; Kulmala, M.; Fu, C. B., Influence of biomass burning plumes on HONO chemistry in eastern China. *Atmos. Chem. Phys.* **2015,** *15*, (3), 1147-1159.
(21) Yang, Y.; Shao, M.; Keßel, S.; Li, Y.; Lu, K.; Lu, S.; Williams, J.; Zhang, Y.; Zeng, L.; Nölscher, A. C.; Wu, Y.; Wang, X.; Zheng, J., How the OH reactivity affects the ozone production efficiency: case studies in Beijing and Heshan, China. *Atmos. Chem. Phys.* **2017,** *17*, (11), 7127-7142.
(22) Liu, C.; Liu, J.; Liu, Y.; Chen, T.; He, H., Secondary organic aerosol formation from the OH-initiated oxidation of guaiacol under different experimental conditions. *Atmos. Environ.* **2019,** *207*, 30-37.
(23) Sarrafzadeh, M.; Wildt, J.; Pullinen, I.; Springer, M.; Kleist, E.; Tillmann, R.; Schmitt, S. H.; Wu, C.; Mentel, T. F.; Zhao, D.; Hastie, D. R.; Kiendler-Scharr, A., Impact of NOx and OH on secondary organic aerosol formation from β-pinene photooxidation. *Atmos. Chem. Phys.* **2016,** *16*, (17), 11237-11248.
(24) Herrmann, H.; Schaefer, T.; Tilgner, A.; Styler, S. A.; Weller, C.; Teich, M.; Otto, T., Tropospheric Aqueous-Phase Chemistry: Kinetics, Mechanisms, and Its Coupling to a Changing Gas Phase. *Chem. Rev.* **2015,** *115*, (10), 4259-4334.
(25) Kroll, J. H.; Ng, N. L.; Murphy, S. M.; Varutbangkul, V.; Flagan, R. C.; Seinfeld, J. H., Chamber studies of secondary organic aerosol growth by reactive uptake of simple carbonyl compounds. *J. Geophys. Res: Atmos.* **2005,** *110*, (D23).
(26) Hallquist, M.; Wenger, J. C.; Baltensperger, U.; Rudich, Y.; Simpson, D.; Claeys, M.; Dommen, J.; Donahue, N. M.; George, C.; Goldstein, A. H.; Hamilton, J. F.; Herrmann, H.; Hoffmann, T.; Iinuma, Y.; Jang, M.; Jenkin, M. E.; Jimenez, J. L.; Kiendler-Scharr, A.; Maenhaut, W.; McFiggans, G.; Mentel, T. F.; Monod, A.; Prévôt, A. S. H.; Seinfeld, J. H.; Surratt, J. D.; Szmigielski, R.; Wildt, J., The formation, properties and impact of secondary organic aerosol: current and emerging issues. *Atmos. Chem. Phys.* **2009,** *9*, (14), 5155-5236.
(27) Seinfeld, J. H., Pandis, S.N, Atmospheric Chemistry and Physics e From Air Pollution to Climate Change, second ed. John Wiley and Sons, Inc., New York, **2006**.
(28) Cao, Y.; Zhang, Z.; Xiao, H.; Xie, Y.; Liang, Y.; Xiao, H., How aerosol pH responds to nitrate to sulfate ratio of fine-mode particulate. *Environ. Sci. Pollut. Res.* **2020,** *27*, (28), 35031-35039.
(29) Jiang, H.; Li, Z.; Wang, F.; Zhou, X.; Wang, F.; Ma, S.; Zhang, X., Water-Soluble Ions in Atmospheric Aerosol Measured in a Semi-Arid and Chemical-Industrialized City, Northwest China. *Atmosphere* **2021,** *12*, (4).
(30) Tilgner, A.; Schaefer, T.; Alexander, B.; Barth, M.; Collett Jr, J. L.; Fahey, K. M.; Nenes, A.; Pye, H. O. T.; Herrmann, H.; McNeill, V. F., Acidity and the multiphase chemistry of atmospheric aqueous particles and clouds. *Atmos. Chem. Phys. Discuss.* **2021,** *2021*, 1-82.
(31) Wang, J.; Li, J.; Ye, J.; Zhao, J.; Wu, Y.; Hu, J.; Liu, D.; Nie, D.; Shen, F.; Huang, X.; Huang, D. D.; Ji, D.; Sun, X.; Xu, W.; Guo, J.; Song, S.; Qin, Y.; Liu, P.; Turner, J. R.;

Lee, H. C.; Hwang, S.; Liao, H.; Martin, S. T.; Zhang, Q.; Chen, M.; Sun, Y.; Ge, X.; Jacob, D. J., Fast sulfate formation from oxidation of SO2 by NO2 and HONO observed in Beijing haze. *Nat. Commun.* **2020,** *11*, (1), 2844.
(32) Shi, G.; Xu, J.; Peng, X.; Xiao, Z.; Chen, K.; Tian, Y.; Guan, X.; Feng, Y.; Yu, H.; Nenes, A.; Russell, A. G., pH of Aerosols in a Polluted Atmosphere: Source Contributions to Highly Acidic Aerosol. *Environ. Sci. Technol.* **2017,** *51*, (8), 4289-4296.
(33) Cheng, Y.; Zheng, G.; Wei, C.; Mu, Q.; Zheng, B.; Wang, Z.; Gao, M.; Zhang, Q.; He, K.; Carmichael, G.; Pöschl, U.; Su, H., Reactive nitrogen chemistry in aerosol water as a source of sulfate during haze events in China. *Sci. Adv.* **2016,** *2*, (12), e1601530.
(34) Qiao, Y.; Feng, J.; Liu, X.; Wang, W.; Zhang, P.; Zhu, L., Surface water pH variations and trends in China from 2004 to 2014. *Environ. Monit. Assess.* **2016,** *188*, (7), 443.
(35) Liu, J.; Li, S.; Mekic, M.; Jiang, H.; Zhou, W.; Loisel, G.; Song, W.; Wang, X.; Gligorovski, S., Photoenhanced Uptake of NO2 and HONO Formation on Real Urban Grime. *Environ. Sci. Technol. Lett.* **2019,** *6*, (7), 413-417.
(36) Liu, J.; Deng, H.; Lakey, P. S. J.; Jiang, H.; Mekic, M.; Wang, X.; Shiraiwa, M.; Gligorovski, S., Unexpectedly High Indoor HONO Concentrations Associated with Photochemical NO2 Transformation on Glass Windows. *Environ. Sci. Technol.* **2020,** *54*, (24), 15680-15688.
(37) Liu, J.; Deng, H.; Li, S.; Jiang, H.; Mekic, M.; Zhou, W.; Wang, Y.; Loisel, G.; Wang, X.; Gligorovski, S., Light-Enhanced Heterogeneous Conversion of NO2 to HONO on Solid Films Consisting of Fluorene and Fluorene/Na2SO4: An Impact on Urban and Indoor Atmosphere. *Environ. Sci. Technol.* **2020,** *54*, (18), 11079-11086.
(38) Yu, Z.; Liu, C.; Niu, H.; Wu, M.; Gao, W.; Zhou, Z.; Huang, Z.; Li, X., Real time analysis of trace volatile organic compounds in ambient air: a comparison between membrane inlet single photon ionization mass spectrometry and proton transfer reaction mass spectrometry. *Anal. Methods* **2020,** *12*, (35), 4343-4350.
(39) Liu, J.; Li, S.; Zeng, J.; Mekic, M.; Yu, Z.; Zhou, W.; Loisel, G.; Gandolfo, A.; Song, W.; Wang, X.; Zhou, Z.; Herrmann, H.; Li, X.; Gligorovski, S., Assessing indoor gas phase oxidation capacity through real-time measurements of HONO and NOx in Guangzhou, China. *Environ. Sci.: Processes Impacts* **2019,** *21*, (8), 1393-1402.
(40) Mekic, M.; Zeng, J.; Jiang, B.; Li, X.; Lazarou, Y. G.; Brigante, M.; Herrmann, H.; Gligorovski, S., Formation of Toxic Unsaturated Multifunctional and Organosulfur Compounds From the Photosensitized Processing of Fluorene and DMSO at the Air-Water Interface. *J. Geophys. Res.: Atmos.* **2020,** *125*, (6), e2019JD031839.
(41) Deng, H.; Liu, J.; Wang, Y.; Song, W.; Wang, X.; Li, X.; Vione, D.; Gligorovski, S., Effect of Inorganic Salts on N-Containing Organic Compounds Formed by Heterogeneous Reaction of NO2 with Oleic Acid. *Environ. Sci. Technol.* **2021,** *55*, (12), 7831-7840.
(42) Cheung, J. L.; Li, Y. Q.; Boniface, J.; Shi, Q.; Davidovits, P.; Worsnop, D. R.; Jayne, J. T.; Kolb, C. E., Heterogeneous Interactions of NO2 with Aqueous Surfaces. *J. Phys. Chem. A* **2000,** *104*, (12), 2655-2662.
(43) Hanson, D. R.; Ravishankara, A. R.; Solomon, S., Heterogeneous reactions in sulfuric acid aerosols: A framework for model calculations. *J. Geophys. Res.: Atmos.* **1994,** *99*, (D2), 3615-3629.
(44) Mekic, M.; Loisel, G.; Zhou, W.; Jiang, B.; Vione, D.; Gligorovski, S., Ionic-Strength Effects on the Reactive Uptake of Ozone on Aqueous Pyruvic Acid: Implications for Air–Sea Ozone Deposition. *Environ. Sci. Technol.* **2018,** *52*, (21), 12306-12315.
(45) Behnke, W.; George, C.; Scheer, V.; Zetzsch, C., Production and decay of ClNO2 from the reaction of gaseous N2O5 with NaCl solution: Bulk and aerosol experiments. *J. Geophys. Res.: Atmos.* **1997,** *102*, (D3), 3795-3804.

(46) Clifford, D.; Donaldson, D. J.; Brigante, M.; D'Anna, B.; George, C., Reactive Uptake of Ozone by Chlorophyll at Aqueous Surfaces. *Environ. Sci. Technol* **2008,** *42*, (4), 1138-1143.
(47) Khudoshin, A. G.; Mitrofanova, A. N.; Lunin, V. V., Lignin transformations and reactivity upon ozonation in aqueous media. *Russ. J. Phys. Chem. A* **2012,** *86*, (3), 360-365.
(48) Finlayson-Pitts, B. J., The Tropospheric Chemistry of Sea Salt: A Molecular-Level View of the Chemistry of NaCl and NaBr. *Chem. Rev.* **2003,** *103*, (12), 4801-4822.
(49) Reeser, D. I.; Jammoul, A.; Clifford, D.; Brigante, M.; D'Anna, B.; George, C.; Donaldson, D. J., Photoenhanced Reaction of Ozone with Chlorophyll at the Seawater Surface. *J. Phys. Chem. C* **2009,** *113*, (6), 2071-2077.
(50) Oldridge, N. W.; Abbatt, J. P. D., Formation of Gas-Phase Bromine from Interaction of Ozone with Frozen and Liquid NaCl/NaBr Solutions: Quantitative Separation of Surficial Chemistry from Bulk-Phase Reaction. *J. Phys. Chem. A* **2011,** *115*, (12), 2590-2598.
(51) Mekic, M.; Brigante, M.; Vione, D.; Gligorovski, S., Exploring the ionic strength effects on the photochemical degradation of pyruvic acid in atmospheric deliquescent aerosol particles. *Atmos. Environ.* **2018,** *185*, 237-242.
(52) Zhou, W.; Mekic, M.; Liu, J.; Loisel, G.; Jin, B.; Vione, D.; Gligorovski, S., Ionic strength effects on the photochemical degradation of acetosyringone in atmospheric deliquescent aerosol particles. *Atmos. Environ.* **2019,** *198*, 83-88.
(53) Mekic, M.; Gligorovski, S., Ionic strength effects on heterogeneous and multiphase chemistry: Clouds versus aerosol particles. *Atmos. Environ.* **2021,** *244*, 117911.
(54) Liu, Y.; Sheaffer, R. L.; Barker, J. R., Effects of Temperature and Ionic Strength on the Rate and Equilibrium Constants for the Reaction I•aq + I-aq ↔ I2•-aq. *J. Phys. Chem. A* **2003,** *107*, (48), 10296-10302.
(55) Guggenheim, E. A.; Wiseman, L. A., Kinetic salt effects on the inversion of sucrose. *Proc. R. Soc. London, Ser. A* **1950,** *203*, (1072), 17-32.
(56) Perlmutter-Hayman, B.; Stein, G., Specific Ionic Effects on Reaction Rates. The Reaction between Persulfate and Iodide Ions in the Presence of High Concentrations of Added Salts. *J. Chem. Phys.* **1964,** *40*, (3), 848-852.
(57) Bao, Z.-C.; Barker, J. R., Temperature and Ionic Strength Effects on Some Reactions Involving Sulfate Radical [SO4-(aq)]. *J. Phys. Chem.* **1996,** *100*, (23), 9780-9787.
(58) Mekic, M.; Zeng, J.; Zhou, W.; Loisel, G.; Jin, B.; Li, X.; Vione, D.; Gligorovski, S., Ionic Strength Effect on Photochemistry of Fluorene and Dimethylsulfoxide at the Air–Sea Interface: Alternative Formation Pathway of Organic Sulfur Compounds in a Marine Atmosphere. *ACS Earth Space Chem.* **2020,** *4*, (7), 1029-1038.
(59) Herrmann, H., Kinetics of Aqueous Phase Reactions Relevant for Atmospheric Chemistry. *Chem. Rev.* **2003,** *103*, (12), 4691-4716.
(60) von Bünau G.; Wolff, T., Photochemie, Grundlagen, Methoden, Anwendungen; VCH Verlagsgesellschaft, Wiley-VCH, Weinheim, Germany, **1987**.
(61) Loisel, G.; Mekic, M.; Liu, S.; Song, W.; Jiang, B.; Wang, Y.; Deng, H.; Gligorovski, S., Ionic strength effect on the formation of organonitrate compounds through photochemical degradation of vanillin in liquid water of aerosols. *Atmos. Environ.* **2021,** *246*, 118140.
(62) Ragnar, M.; Lindgren, C. T.; Nilvebrant, N.-O., pKa-Values of Guaiacyl and Syringyl Phenols Related to Lignin. *J. Wood Chem. Technol.* **2000,** *20*, (3), 277-305.
(63) Prütz, W. A.; Mönig, H.; Butler, J.; Land, E. J., Reactions of nitrogen dioxide in aqueous model systems: Oxidation of tyrosine units in peptides and proteins. *Arch. Biochem. Biophys.* **1985,** *243*, (1), 125-134.

(64) Rubio, M. A.; Lissi, E.; Olivera, N.; Reyes, J. L.; López-Alarcon, C., Reactions of p-Substituted Phenols with Nitrous Acid in Aqueous Solution. *Int. J. Chem. Kinet.* **2014,** *46*, (3), 143-150.
(65) Angle, K. J.; Crocker, D. R.; Simpson, R. M. C.; Mayer, K. J.; Garofalo, L. A.; Moore, A. N.; Mora Garcia, S. L.; Or, V. W.; Srinivasan, S.; Farhan, M.; Sauer, J. S.; Lee, C.; Pothier, M. A.; Farmer, D. K.; Martz, T. R.; Bertram, T. H.; Cappa, C. D.; Prather, K. A.; Grassian, V. H., Acidity across the interface from the ocean surface to sea spray aerosol. *Proc. Nat. Acad. Sci.* **2021,** *118*, (2), e2018397118.
(66) Arens, F.; Gutzwiller, L.; Gäggeler, H. W.; Ammann, M., The reaction of NO2 with solid anthrarobin (1,2,10-trihydroxy-anthracene). *Phys. Chem. Chem. Phys.* **2002,** *4*, (15), 3684-3690.
(67) Nah, T.; Kessler, S. H.; Daumit, K. E.; Kroll, J. H.; Leone, S. R.; Wilson, K. R., OH-initiated oxidation of sub-micron unsaturated fatty acid particles. *Phys. Chem. Chem. Phys.* **2013,** *15*, (42), 18649-18663.
(68) Zhang, X.; Barraza, K. M.; Upton, K. T.; Beauchamp, J. L., Time resolved study of hydroxyl radical oxidation of oleic acid at the air-water interface. *Chem. Phys. Lett.* **2017,** *683*, 76-82.
(69) Huang, Z.; Noble, B. B.; Corrigan, N.; Chu, Y.; Satoh, K.; Thomas, D. S.; Hawker, C. J.; Moad, G.; Kamigaito, M.; Coote, M. L.; Boyer, C.; Xu, J., Discrete and Stereospecific Oligomers Prepared by Sequential and Alternating Single Unit Monomer Insertion. *J. Am. Chem. Soc.* **2018,** *140*, (41), 13392-13406.
(70) Zeng, J.; Mekic, M.; Xu, X.; Loisel, G.; Zhou, Z.; Gligorovski, S.; Li, X., A Novel Insight into the Ozone–Skin Lipid Oxidation Products Observed by Secondary Electrospray Ionization High-Resolution Mass Spectrometry. *Environ. Sci. Technol.* **2020,** *54*, (21), 13478-13487.
(71) Zhang, Q.; Shen, Z.; Zhang, L.; Zeng, Y.; Ning, Z.; Zhang, T.; Lei, Y.; Wang, Q.; Li, G.; Sun, J.; Westerdahl, D.; Xu, H.; Cao, J., Investigation of Primary and Secondary Particulate Brown Carbon in Two Chinese Cities of Xi'an and Hong Kong in Wintertime. *Environ. Sci. Technol.* **2020,** *54*, (7), 3803-3813.
(72) Bedini, A.; Maurino, V.; Minero, C.; Vione, D., Theoretical and experimental evidence of the photonitration pathway of phenol and 4-chlorophenol: A mechanistic study of environmental significance. *Photochem. Photobiol. Sci.* **2012,** *11*, (2), 418-424.
(73) Bianchi, F.; Kurten, T.;́ Riva, M.; Mohr, C.; Rissanen, M. P.; Roldin, P.; Berndt, T.; Crounse, J.D.; Wennberg, P.O.; Mentel, T.F.; Wildt, J.; Junninen, H.; Jokinen, T.; Kulmala, M.; Worsnop, D. R.;. Thornton, J.A.; Donahue, N.; Kjaergaard, H.G.; Ehn, M. Highly Oxygenated Organic Molecules (HOM) from Gas-Phase Autoxidation Involving Peroxy Radicals: A Key Contributor to Atmospheric Aerosol. *Chem. Rev.* **2019**, *119*, 3472−3509.